Microstructure of Polyfuran/Perchlorate-Doped Films by Scanning and Transmission Electron Microscopies and Electron Diffraction

I. Carrillo,[†] C. Barba,[‡] M. J. González-Tejera,[†] and I. Hernández-Fuentes*[,†]

Facultad de Ciencias Químicas, Departamento de Química Física I, and Centro de Microscopía Electrónica, Universidad Complutense, 28040 Madrid, Spain

Received January 22, 1996; Revised Manuscript Received May 23, 1996[⊗]

ABSTRACT: Polyfuran films doped with perchlorate anions (PFu/ClO_4) were studied by scanning and transmission electron microscopies and electron diffraction in order to analyze their morphology and microstructure. Film generation was carried out electrochemically at constant potential, $E_d = 2.6$ V (Ag/Ag^+), onto platinum electrodes in acetonitrile/sodium perchlorate medium. The study of the superficial films morphology revealed an ordered nodular structure in the films growth face, the nodular size depending on E_d. Alignment of nodules followed a direction parallel to the substrate. Crystalline structures immersed in amorphous domains were found in planar sections and cross-sections of PFu/ClO_4 films by transmission electron microscopy and selected area micro-electron diffraction. Planar sections close to the film growth surface exhibited randomly oriented crystals, while single crystals with lamellar structures were detected in deeper layers. Electron diffraction patterns obtained in planar and transversal sections were consistent with a hexagonal unit cell: $a = 0.68$ nm and $c = 0.62$ nm, $\alpha = \beta = 90°$, and $\gamma = 120°$. The existence of moiré patterns in planar sections confirms the laminar structure proposed for PFu/ClO_4 films.

Introduction

During the 1990s remarkable progress has been made in the field of doped polyfuran films. Previously, due to the difficulties of synthesis,[1−4] all efforts were concentrated on other conducting polymers such as polyacetylene, polyaniline, polypyrrole, polythiophene, etc. Research into the morphology and internal structure of all these materials is at an early stage, but information about microstructural organization of conducting polymers is important for interpreting their macroscopic properties. Most studies concerning film growth have focused on scanning electron microscopy analysis. These studies have proved very useful for establishing surface morphology but not microstructure. Owing to the lack of bulk crystallinity in most of the electrodeposited conducting films and the difficulties of sample preparation for transmission electron microscopy (TEM) and electron or X-ray diffraction, little use has been made of these techniques; scanning tunneling and atomic force microscopies having proved more effective.[5,6] Another problem that makes these studies difficult is the polymer sensitivity to radiation damage. The effect of electron irradiation on polypyrrole, for instance, is quite important, with loss of order occurring in some cases after 5 or 10 min of beam exposure.[7] Nevertheless, some recent works try to analyze the growth and structure of conducting polymers by these techniques.[7−12] Yamamoto et al.[8] have studied the influence of the substrate temperature, strength of interaction between the polymer and the substrates, and linearity of the polymer molecules on the level of order in highly oriented crystalline thin films obtained by vacuum evaporation of π-conjugated systems, poly(*p*-phenylene), poly(thiophene-2,5-diyl), and poly(2,2′-bipyridine-5,5′-diyl) on carbon substrates. Likewise, the solvent influence on the development of supramolecular ordering within PPy-doped films has been developed by scanning electron microscopy (SEM), TEM, polarizing optical microscopy, and wide-angle X-ray scattering.[7,9] On the other hand, the rearrangement of the individual molecules has been analyzed on polyaniline[10] by TEM and X-ray diffraction supporting the conductive islands concept proposed by Epstein et al.[11] Differences have been observed between electron diffraction patterns of undoped polymer and those of oriented regions of doped cis polyacetylene.[12]

Synthesis of stable, electroactive doped polyfuran films by anodic coupling of furan has long been delayed by the high oxidation potential of the monomer.[13] A systematic study of the influence of deposition potential on potentiostatic generation,[3,4] aromaticity,[14] and morphology[15] of perchlorate-doped polyfuran films (PFu/ClO_4) has been published recently. SEM analysis revealed an ordered nodular structure in those films never before observed in other conducting polymers doped with the same or different anions.[15] Thus, polypyrrole films doped with perchlorate anions present a cauliflower-like appearance[16−18] (in this connection, fractal analysis of polypyrrole deposits has recently been developed[19,20]). Also, owing to the versatility of preparation methods, polyaniline exhibits variable morphology generally described as either granular or fibrous.[21−23]

To the best of our knowledge, no polyfuran morphological studies by transmission electron microscopy and electron diffraction have been published. The scope of this work was to screen the surface morphology and the microstructure of PFu/ClO_4 films by scanning and transmission electron microscopies and selected area micro-electron diffraction of planar and transversal sections of the films.

Experimental Section

PFu/ClO_4 Film Electrogeneration. PFu/ClO_4 films were potentiostatically generated onto platinum electrodes at a deposition potential $E_d = 2.6$ V (Ag/Ag^+) and during a deposition time $t_d = 600$ s. For this purpose, a Princeton Applied Research potentiostat/galvanostat Model 273A was used.

* To whom all correspondence should be addressed.
† Departamento de Química Física I.
‡ Centro de Microscopía Electrónica.
⊗ Abstract published in *Advance ACS Abstracts,* July 1, 1996.

S0024-9297(96)00101-5 CCC: $12.00

The electrochemical growth of PFu/ClO_4 films was carried out in a single compartment, three-electrode cell under a nitrogen atmosphere at room temperature. The nonaqueous electrolyte medium consisted of acetonitrile (MeCN, Carlo Erba, RPE quality) dried over 3 Å molecular sieves and sodium perchlorate ($NaClO_4$, Aldrich Chemie, 99%). The monomer furan (Fu, Aldrich Chemie, 99%) was distilled under vacuum before use. The electropolymerization solutions contained 0.1 M Fu and 0.1 M $NaClO_4$ in MeCN.

Platinum working electrodes were not treated in any way as to produce specific orientation. They were polished first with alumina and, afterward, with diamond paste, cleaned in acetone in an ultrasonic bath, then washed with water and hot concentrated sulfuric acid, and finally rinsed copiously with Milli-Q water and dried. After that, the final surface electrode area was checking by scanning electron microscopy to test its smoothness, avoiding the existence of polishing rows.

A roughnessmeter device Dectak3 was used to determine the film surface roughness.

Scanning Electron Microscopy. Scanning electron micrographs were obtained on a JEOL Model JSM 6400 electron microscope at 20 kV and varying levels of magnification. For this purpose, PFu/ClO_4 films were peeled back from the platinum electrode and glued with graphite paste to a copper holder. Then, they were coated by sputtering with a thin gold film to avoid charge buildups because of their low conductivity, and both faces and the cross-section, which corresponded to a transverse fracture of the film, were examined. No metalization effects on the morphology of these films were observed. Before coating, samples were examined at 5 kV acceleration potential voltage to minimize the charge buildups, good correspondence being obtained among images before (at 5 kV) and after coating (at 20 kV).

A Videoplan image program was used to determine the average area and perimeter of the nodules of the film surface.

Transmission Electron Microscopy and Electron Diffraction. Transmission electron microscopy (TEM) and electron diffraction (ED) were carried out on a JEOL Model JEM 2000 FX electron microscope at 200 kV, the selected area microdiffraction method being used. For local observations with TEM, the first step was to obtain ultrathin sections by ultramicrotomy. Sample preparation was an important factor in the development of such experiments. Prior to sectioning, samples were embedded in an epoxy resin (Epon 812) and cured at 70 °C for 72 h to obtain parallel and perpendicular cuts to the film surfaces. Ultramicrotome sections, 50 nm thick, were cut with diamond knives in a Reichert Model Ultracut E ultramicrotome at room temperature using standard procedures. These sections, floated off onto the surface of distilled water, were chosen according to their interference color in reflected light and picked up on cooper grids (100 or 200 mesh size). All grids were coated with a thin layer of carbon graphite to improve heating conductivity.

The illumination conditions were carefully chosen in order to image the crystals before their destruction. TEM micrographs were obtained after the diffraction. Focus conditions were tested first in an adjacent zone in order to avoid damage to our crystalline zones from the beam. No visible alterations in polymer structure were observed during the ED and TEM viewing and photographic process.

The TEM bright field images were recorded on Agfa Scientia EM films through either a 50 or 80 μm objective aperture with magnifications ranging from 8×10^4 to 15×10^4. The spot size was 40 nm. All TEM images were properly orientated with respect to the diffraction pattern.

TEM images and ED patterns of cross-sections and planar sections at different depths were confirmed using both different PFu/ClO_4 films synthesized in the conditions previously described and different crystals in each section of the films.

Results and Discussion

Scanning electron microscopy has been primarily used to investigate the surface topography of PFu/ClO_4 films and to analyze the bulk morphology by viewing cross-sections of the films corresponding to transverse fractures.

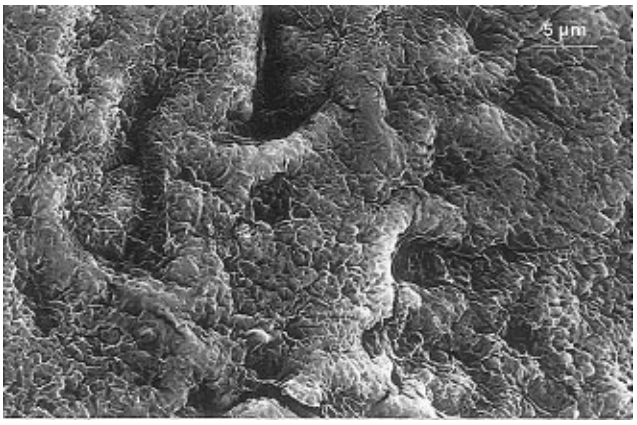

Figure 1. Scanning electron micrograph of the back face of PFu/ClO_4 films.

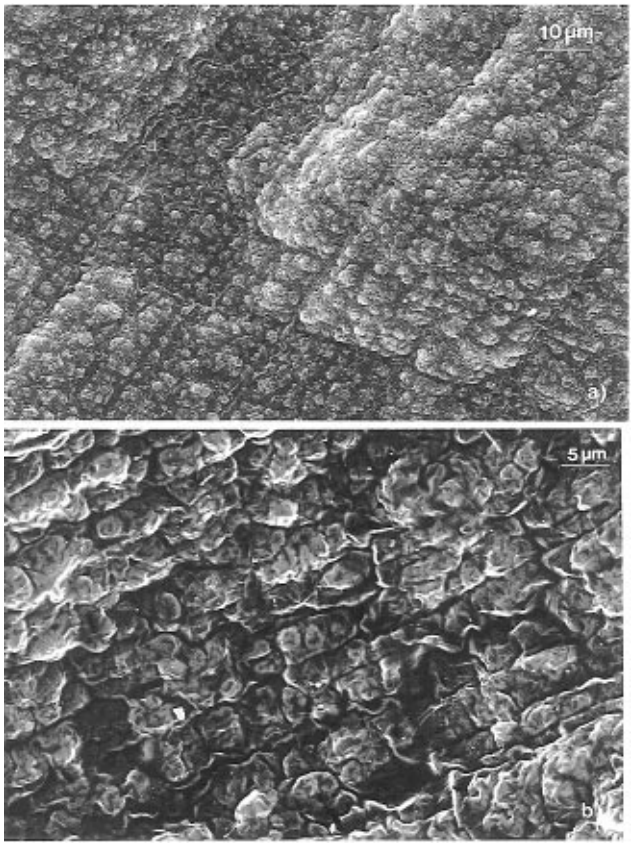

Figure 2. Scanning electron micrographs of the growth face of PFu/ClO_4 films at two different magnifications.

Figures 1 and 2 show the scanning electron micrographs of both faces of PFu/ClO_4 films generated at 2.6 V (Ag/Ag^+). The back face of the films (surface facing the platinum electrode during film generation) (Figure 1) was shiny, smoother, and more homogeneous than the growth face (face in contact with the solution during the film electrogeneration) which was matte and quite regular. The latter exhibited an ordered interlinked nodular structure oriented 45° to the lengthwise axis of the electrode over the entire sample surface (see Figure 2a and 2b); similar structures have been reported for PFu/ClO_4 films obtained by the same procedure but in other conditions of synthesis.[4,15] Average area and perimeter values of nodules calculated, taking care to prevent nodule interpenetration, were 1.19 ± 0.07 μm^2

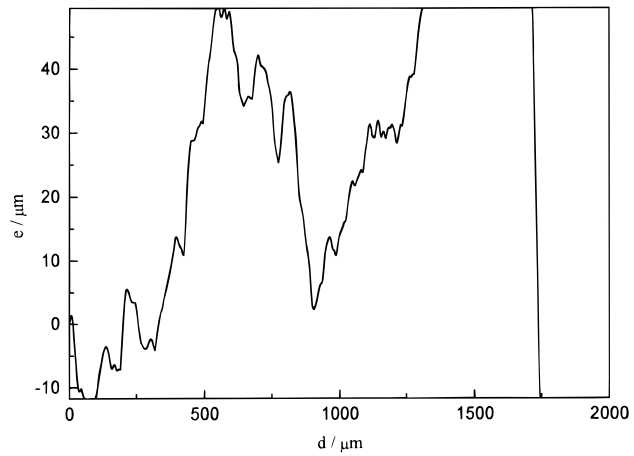

Figure 3. Roughness profile of the growth face of PFu/ClO_4 films.

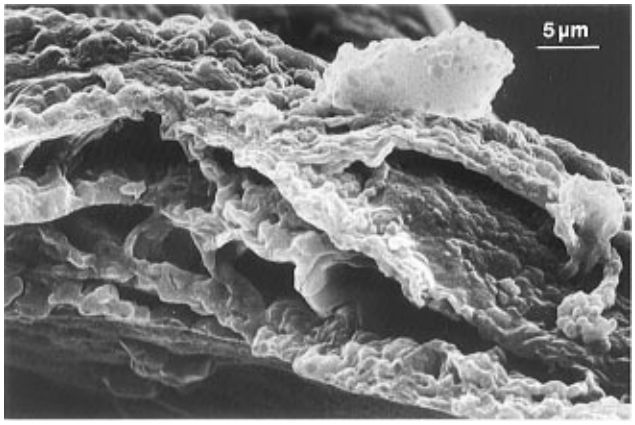

Figure 4. Scanning electron micrograph of a cross-section of PFu/ClO_4 films.

and 3.79 ± 0.13 μm, respectively. The Kolmogorov-Smirnov test[24] showed that a normal distribution function could be assumed for these magnitudes. The comparison of the nodules of PFu/ClO_4 films synthesized at the same concentration conditions but different deposition potentials[4] indicated that nodule size decreased as E_d rose.

Different levels of growth in PFu/ClO_4 films were observed in Figure 2a, lending these films a rough appearance and maintaining the ordered nodular structure. This feature was confirmed from the film roughness profile (see Figure 3), in which differences of thickness greater than 60 μm were detected in 2 mm of scanning length. This roughness could be caused by the nonsimultaneous nucleation over the entire electrode surface in the course of film electrogeneration, which began at the edges and rapidly spread inward, completely covering the platinum surface (at the same time as nucleation took place in some parts of the electrode, film grew over the previously-formed nuclei in other areas). The SEM image of the film cross-section (Figure 4) suggested that an additional cause of roughness could be alternating planar and normal growth of the film; this could account for the porous texture of the bulk morphology of PFu/ClO_4 films, which was composed of interlinked nodular layers with some intervening cavities.

The transmission electron micrograph of a superficial planar section, cut parallel to the growth surface of PFu/ClO_4 films, and its corresponding electron diffraction pattern, are shown in Figure 5. The TEM image (Figure 5a) revealed the presence of crystals in different layers near the sample border, which are indicated by an arrow. Their random orientation is responsible for the concentric ring diffraction pattern observed in Figure 5b. In the diffraction patterns 13 reciprocal lattice signals, which are listed in Table 1, can be seen. There are three strong diffraction signals at 0.586, 0.341, and 0.293 nm in the real space, that can be observed clearly in Figure 5b. The weaker reflections, not visible in the print, are sketched in Figure 5c. The eight signals

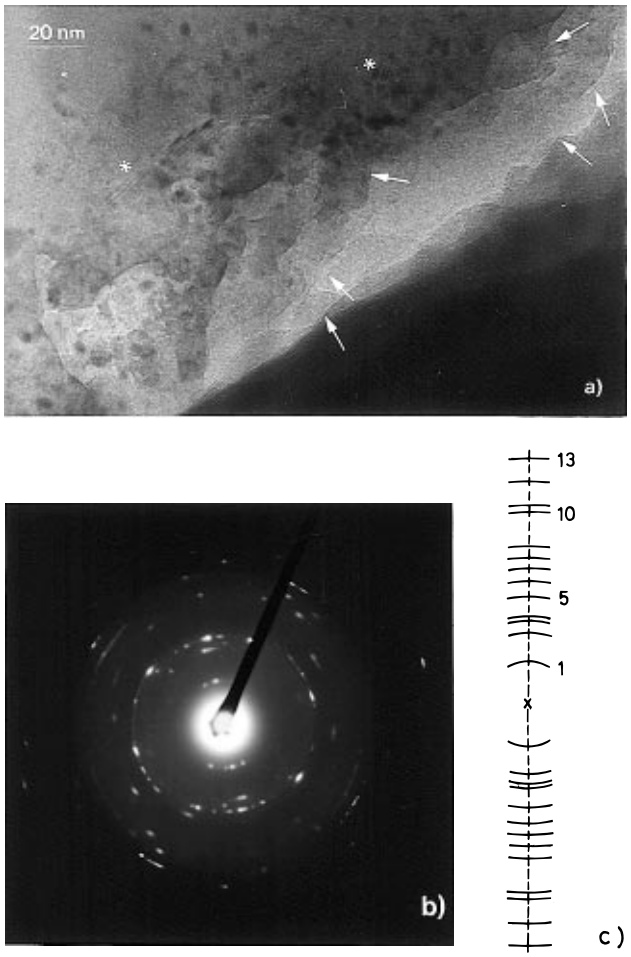

Figure 5. (a) Transmission micrograph of a superficial planar section of PFu/ClO_4 films. Crystals and lamellar structures are indicated with an arrow and an asterisk, respectively. (b) Corresponding electron diffraction pattern. (c) Sketch of the diffraction pattern to show the weaker reflections not visible on the print. The numbers refer to Table 1.

Table 1. Observed and Calculated Electron Diffraction Spacings of Concentric Rings Based on the Electron Diffraction Pattern Shown in Figure 5b

	measd spacing/nm	intensity[a]	index	calcd spacing/nm
1	0.586	s	(100)	0.588
2	0.341	s	(110)	0.340
3	0.315	m	(002)	0.310
4	0.293	s	(200)	0.294
5	0.278	m	(102)	0.275
6	0.229	m-s	(210)	0.226
7	0.197	m	(300)	0.196
8	0.182	m	(212)	0.181
9	0.170	m	(220)	0.170
10	0.158	w	(311)	0.158
11	0.129	w	(410)	0.128
12	0.111	w	(420)	0.111
13	0.101	vw	(225)	0.100

[a] s = strong, m = medium, w = weak, vw = very weak.

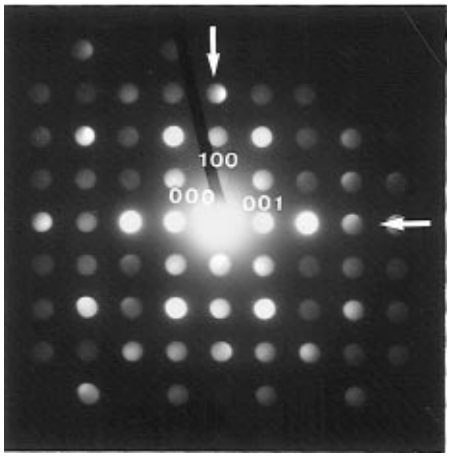

Figure 6. Electron diffraction pattern of a cross-section of PFu/ClO_4 films.

indexed as $hk0$ reflections are more defined in a preferential direction and correspond to the hexagonal system,[25] the a-axis being 0.68 nm. The remaining signals in Table 1 could be assigned to other l values in the hexagonal system after obtaining the c-axis.

In order to determine the c-axis of the hexagonal unit cell, the diffraction pattern of a cross-section has been used. This pattern consisting of $h0l$ reflections with different intensities is shown in Figure 6, perpendicular a^* and c axes being marked with arrows. The reflections along a^* and c at 0.59 and 0.62 nm are indexed as (100) and (001), respectively. Therefore, the unit cell constants of PFu/ClO_4 films in real space could be established as $a = 0.68$ nm and $c = 0.62$ nm, $\alpha = \beta = 90°$, and $\gamma = 120°$. These parameters allowed us to index all the diffraction patterns found in different fragments of different PFu/ClO_4 films synthesized in the same conditions.

In Figure 7 the TEM micrograph and its corresponding ED pattern of a deeper planar section of a PFu/ClO_4 film can be seen. The TEM micrograph (Figure 7a) reveals some crystals superimposed on one another, indicating a laminar structure with some preferential directions. The image also shows an alternating sequence of dark and light lines with different orientations which correspond to the typical features of the lamellar structure. The dark regions correspond to the crystal core, and the light bands, to the disordered or amorphous lamellar surface and interlamellar material. The lamellea were not uniformly distributed along the TEM micrograph and were constituted by a variable number of repeating lamellae units, from four to seven. The individual lamellae of consistent thickness has a spacing from 11 to 18 nm. It is interesting to mention that in superficial planar sections (Figure 5a), a small contribution of lamellar structure (marked with asterisks) is observed.

The ED pattern of crystals from deeper planar sections rendered well-defined diagrams with six reflections hexagonally arranged (see Figures 7b). The existence of these well-defined spots indicates that they are single crystals. The (300) and (030) reflections could be seen in this figure, the distances and angle being $d_{030} = d_{300} = 0.196$ nm and $\alpha = 60°$.

Figure 8a shows the electron diffraction pattern of another deep planar section in which some spots with different relative intensities forming a hexagonal pattern can be observed. The sharp spots give a principal hexagonal diffraction pattern equal to the one shown

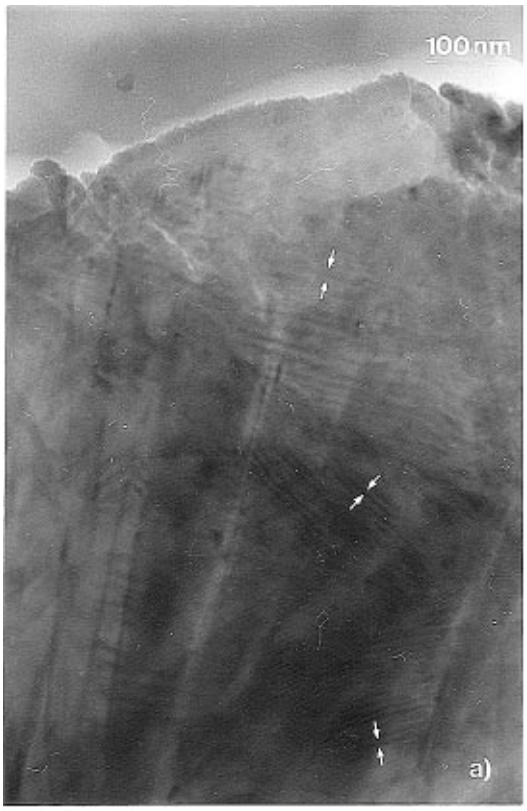

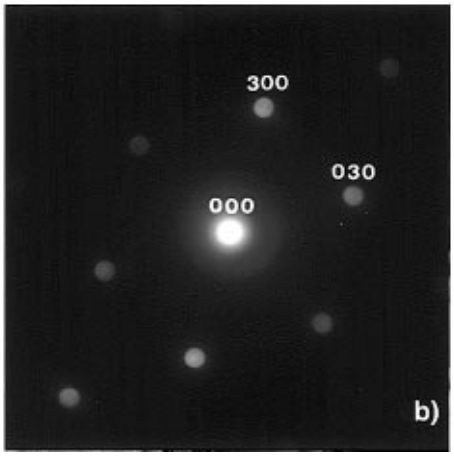

Figure 7. (a) Transmission electron micrograph of a deep planar section of PFu/ClO_4 films. Evidence for lamellae can be identified (arrows). (b) Corresponding electron diffraction pattern.

in Figure 7b. In addition to the strong principal spots, another three weak spots appear, which are sketched in Figure 8b. This ED pattern reveals the existence of a rotation moiré pattern, confirming the laminar structure of our PFu/ClO_4 films.

It is interesting to remark that diffraction patterns similar to the one observed in Figure 7b were also present in cross-sections, but the crystalline zones were in a smaller proportion than in the planar sections. Therefore, crystallinity of the cross-sections was qualitatively lower.

The presence of many crystals with different orientations in the most superficial layers of the films and of single crystals with lamellar structures in deeper layers could be caused by better development of crystallinity in the last ones and, as previously suggested, alternative planar and normal film growth.

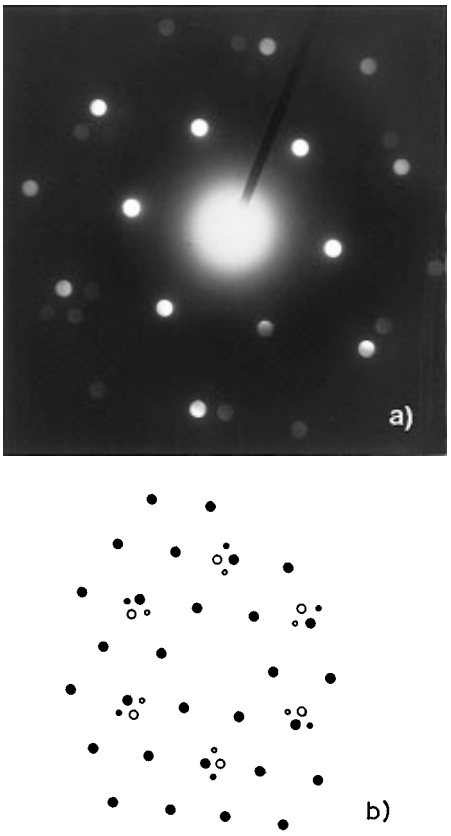

Figure 8. (a) Electron diffraction pattern of another deep planar section of PFu/ClO_4 films. (b) Sketch of the rotation moiré pattern to show the weaker reflections not visible on the print. Large open and closed circles represent primary diffraction spots. Smallest dots represent double-diffraction spots.

Conclusions

In this work, the presence of crystalline microdomains in ordered PFu/ClO_4 films was established by TEM and ED. The growth face of these films, less homogeneous than the back one, showed, by SEM, an ordered nodular structure oriented 45° to the lengthwise axis of the electrode, nodule size diminishing as the deposition potential rose. Their porous bulk morphology was a consequence of the interlinked laminar structure produced by the alternative planar and normal film growth and also by its no simultaneous nucleation process. This kind of film formation could be responsible for the nonuniform bulk crystallinity of PFu/ClO_4 films. Internal layers displayed a more consistent orientation by the existence of bigger single crystals with lamellar structures; however, as the film grew, randomly oriented crystals were produced, being indexed in all film extensions in the hexagonal system. Nevertheless, crystalline domains were in less proportion than amorphous ones.

Acknowledgment. This work has been partially supported by the DGICYT, under project PB92-0188. Thanks are due to Prof. T. Rodriguez and Dr. C. González-Bris (E.T.S.I. Telecomunicación, Universidad Politécnica de Madrid) for helping us in the rugosity measurements.

References and Notes

(1) Zotti, G.; Schiavon, G.; Commiso, N.; Berlin, A.; Pagani, G. *Synth. Met.* **1990**, *36*, 337.
(2) Glenis, S.; Benz, M.; LeGoff, E.; Schindler, J. L.; Kannewurf, C. R.; Kanatzidis, M. G. *J. Am. Chem. Soc.* **1993**, *115*, 12519.
(3) González-Tejera, M. J.; Carrillo, I.; Hernández-Fuentes, I. *An. Quím.* **1993**, *89*, 521.
(4) González-Tejera, M. J.; Carrillo, I.; Hernández-Fuentes, I. *Synth. Met.* **1995**, *73*, 135.
(5) Chao, F.; Costa, M.; Tian, C. *Synth. Met.* **1993**, *53*, 127.
(6) Bai, C.; Zhu, C.; Huang, G.; Yang, J.; Wan, M.; Chen, R. *Ultramicroscopy* **1992**, *42−44*, 1079.
(7) Minto, G. D. G.; Vaughan, A. S. *J. Mater. Sci.* **1995**, *30*, 6028.
(8) (a) Yamamoto, T.; Mori, C.; Wakayama, H.; Zhou, Z.; Maruyama, T.; Ohki, R.; Kanbara, T. *Chem. Lett.* **1991**, 1483. (b) Yamamoto, T.; Morita, A.; Miyazaki, Y.; Maruyama, T.; Wakayama, H.; Zhou, Z.; Nakamura, Y.; Kanbara, T. *Macromolecules* **1992**, *25*, 1214. (c) Yamamoto, T.; Maruyama, T.; Zhou, Z.; Ito, T.; Fukuda, T.; Yoneda, Y.; Begum. F.; Ikeda, T.; Sasaki, S.; Takezoe, H.; Fukuda, A.; Kubota, K. *J. Am. Chem. Soc.* **1994**, *116*, 4832. (d) Yamamoto, T. *Prog. Polym. Sci.* **1992**, *17*, 1153.
(9) Sutton, S. J.; Vaugham, A. S. *Polymer* **1995**, *36*, 1849.
(10) (a) Lux, F.; Hinrichsen, G.; Krinchnyi, V. I.; Nazarova, I. B.; Cheremisow, S. D.; Pohl, M. M. *Synth. Met.* **1993**, *55*, 347. (b) Lux, F.; Hinrichsen, G.; Pohl, M. M. *J. Polym. Sci.* **1994**, *32*, 1957.
(11) (a) Epstein, A. J.; MacDiarmid, A. G.; Pouget, J. P. *Phys. Rev. Lett.* **1990**, *65*, 664. (b) Epstein, A. J.; MacDiarmid, A. G. *Mol. Cryst., Liq. Cryst.* **1988**, *160*, 165.
(12) Chien, J. C. W.; Karasz, F. E.; Shimamura, H. *Macromolecules* **1982**, *15*, 1012.
(13) Tourillon, G.; Garnier, F. *J. Electroanal. Chem.* **1982**, *135*, 173.
(14) Carrillo, I.; Sánchez de la Blanca, E.; González-Tejera, M. J.; Hernández-Fuentes, I. *Chem. Phys. Lett.* **1994**, *229*, 633.
(15) Carrillo, I.; González-Tejera, M. J.; Hernández-Fuentes, I.; Barba, C. *Solid State Commun.* **1995**, *95*, 107.
(16) Otero, T. F.; de Larreta, E. *Synth. Met.* **1988**, *26*, 79.
(17) Vork, F. T. A.; Schuermans, B. C. A. M.; Barendrecht, E. *Electrochim. Acta* **1990**, *35*, 567.
(18) Chiu, H. T.; Lin, J. S.; Huang, C. M. *J. Appl. Electrochem.* **1992**, *22*, 358.
(19) Atchison, S. N.; Burford, R. R.; Darragh, T. A. *Polym. Int.* **1991**, *26*, 261.
(20) Maddison, D. S. *Synth. Met.* **1993**, *55−57*, 3544.
(21) Taguchi, S.; Tanaka, T. *J. Power Sources* **1987**, *20*, 249.
(22) Huang, W. S.; Humphrey, B. D.; MacDiarmid, A. G. *J. Electroanal. Chem.* **1989**, *262*, 289.
(23) Desilvestro, J.; Scheifele, W. *J. Mater. Chem.* **1993**, *3*, 263.
(24) Press, W. H.; Flannery, B. P.; Teukolsky, S. A.; Vetterling, W. T. *Numerical Recipes in C. The Art of Scientific Computing*; Cambridge University Press: New York, 1988.
(25) Edington, J. W. *Electron Diffraction in the Electron Microscope*; Philips: Eindhoven, 1975.

MA960101A